

COMPUTATIONAL MOLECULAR DOCKING, VOLTAMMETRIC
AND SPECTROSCOPIC DNA INTERACTION STUDIES OF
9*N*-(FERROCENYLMETHYL)ADENINEElhafnaoui Lanez^{1, 2}, Lazhar Bechki², Touhami Lanez^{1, *}<https://doi.org/10.23939/chcht13.01.011>

Abstract. The binding free energy of 9*N*-(ferrocenylmethyl)adenine (FMA) with double-stranded deoxyribonucleic acid (DNA) was measured in solution using cyclic voltammetry and electronic spectroscopy (UV-Vis) techniques under similar conditions. The obtained results were confirmed by computational molecular docking. The docking studies yield good approximation with experimental data and showed that the ligand FMA is placed in the minor groove of DNA.

Keywords: DNA, free binding energy, AutoDock, size of binding site, diffusion coefficient.

1. Introduction

Soon after the discovery of ferrocene in 1951 [1, 2] and the determination of its structure one year later [3], it quickly attracted attention of many researchers leading to the synthesis of a wide range of its derivatives. Today, over 600 research reports are published annually on ferrocene and its derivatives.

Due to the ease of functionalization of ferrocene, its derivatives have found many applications in medicinal chemistry, such as antitumor [4-6], anti-HIV [7, 8], anti-malarial [9], antifungal [10], cytotoxic compounds [11, 12], and for deoxyribonucleic acid (DNA) cleavage [13, 14].

Anticancer activity of ferrocene and its derivatives has been largely studied [15-17]; they can bind with the DNA *via* both covalent and noncovalent modes of interactions. Ferrocene and its derivatives are known to exhibit antitumour activity despite the obvious lack of unoccupied co-ordination [18-20]. As a result, the mode of interaction for this group of derivatives could engage non-covalent interactions with DNA. Such interactions might be modified due to functionalization of ferrocenyl group. The ease of functionalising ferrocene and its

derivatives offers substantial range for the design of organometallic derivatives able to noncovalent binding to DNA or any other bioreceptor. Due to their amphoteric nature, there are few examples of ferrocene based adenines being used as novel class of redox-active ligands [21]; however, they are barely explored as DNA binders [22]. Considering developing interest in biologically active ferrocene-nucleobases compounds, we have become interested in the synthesis of 9*N*-(ferrocenylmethyl)adenine. Our interest in 9*N*-(ferrocenylmethyl)adenine and related compounds arose from the fact that until now a few studies have been carried out on their interaction with DNA and on their anti-cancer activities [22].

Cancer can be cured by slowing the quick propagation of cancer cells, which can be achieved either by radiotherapy, *via* reactive oxygen species, or by chemotherapy, using chemical substances that can interact with DNA. Chemotherapy is the treatment of cancer with anticancer drugs; it can be performed by the interaction of DNA binding ligands which may dysfunction it either by strand scission or chain breaking or local unwinding of its double helical structure, leading to destruction of cancer cells. The study of ligand–DNA interaction is essential for understanding the mechanism of ligand action [16]. Such interactions are studied by a diversity of analytical techniques like cyclic voltammetry, electronic spectroscopy, fluorescence, infrared and nuclear magnetic resonance spectroscopy [23-26].

In an attempt to find efficient DNA binders and as per our interest in ferrocene derivatives, we synthesized a potential anti-cancer 9*N*-(ferrocenylmethyl)adenine and investigated its interaction with DNA by cyclic voltammetry, electronic spectroscopy and molecular docking.

2. Experimental

2.1. Chemicals and Reagents

All the chemicals were of analytical grade and were used without further purification.

¹ University of El Oued, VTRS Laboratory, B.P.789, 39000, El Oued, Algeria

² University of Ouargla, Chemistry Department, PO Box 511, 30000, Ouargla, Algeria

* touhami-lanez@univ-eloued.dz

© Lanez E., Bechki L., Lanez T., 2019

2.2. Synthesis

9*N*-(Ferrocenylmethyl)adenine was synthesized cleanly and in moderate yield from the reaction of the well-known quaternary salt *N,N,N*-trimethylammoniomethylferrocene iodide [27] and adenine (Fig. 1). The compounds gave analytical data in accordance with reported methods [22, 28].

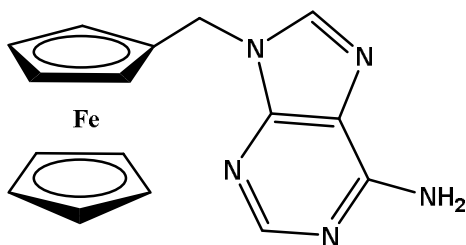


Fig. 1. Structure of 9*N*-(ferrocenylmethyl)adenine

2.3. DNA extraction

DNA was extracted from chicken blood by Falcon method [29]. Ratio of the absorbance of DNA at $\lambda = 260$ nm (A_{260}) and $\lambda = 280$ nm (A_{280}) was used to determine the purity of DNA. The obtained ratio of (A_{260})/(A_{280}) in DNA sample was 1.97, indicating the purity of DNA [30]. The DNA concentration was determined by UV absorbance at 260 nm using the molar extinction coefficient of $6600 \text{ M}^{-1} \cdot \text{cm}^{-1}$ [31].

2.4. Apparatus and Procedures

CV experiments were carried out on a PGZ301 potentiostat/galvanostat (Radiometer Analytical SAS, France) using a three-electrode electrochemical cell of 25 ml containing a glassy carbon (GC) working electrode with a geometric area of 0.013 cm^2 , a platinum wire as counter (auxiliary) and Hg/Hg₂Cl₂ paste covered wire as reference electrode. The voltammogram of 500 μM of FMA in 0.1M aqueous buffer phosphate solution ($\text{KH}_2\text{PO}_4/\text{K}_2\text{HPO}_4$) at pH 7.2 was firstly obtained in the absence of DNA. The voltammograms were then recorded in the presence of an increasing concentration of DNA at 298 K.

Electronic spectra measurements were conducted on a UV-Vis spectrometer, (Shimadzu 1800, Japan). The spectroscopic response of 1mM of FMA in 0.1M aqueous buffer phosphate solution ($\text{KH}_2\text{PO}_4/\text{K}_2\text{HPO}_4$) at pH 7.2 was first recorded at 298 K and then in the presence of gradually increasing concentration of DNA solution.

3. Results and Discussion

3.1. Voltammetric Studies

3.1.1. Binding constant and binding free energy

Determination of the binding constant and binding free energy of FMA with DNA was achieved by recording the voltammograms of the ligand FMA in 0.1M aqueous buffer phosphate solution ($\text{KH}_2\text{PO}_4/\text{K}_2\text{HPO}_4$) at pH 7.2. The cyclic voltammogram of FMA shows an oxidation maximum at 0.338 V and reduction maximum at 0.056 V in a reversible electrochemical process. When an amount of DNA solution was added there was a decrease in anodic peak current with a positive shift in oxidation peak potential. The obtained voltammograms are presented in Fig. 2.

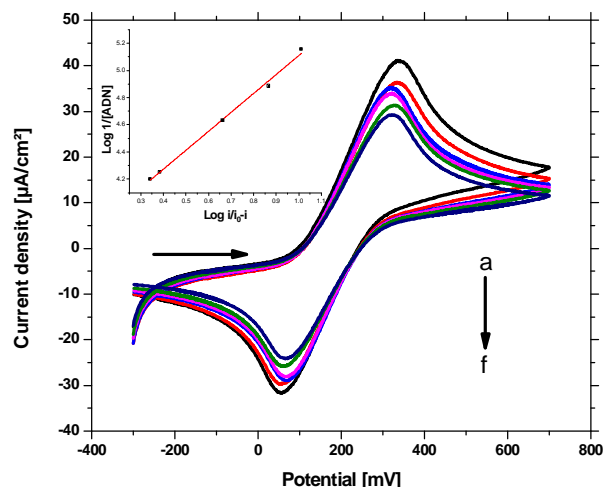


Fig. 2. Cyclic voltammograms of 500 μM FMA in 0.1M buffer phosphate solution ($\text{KH}_2\text{PO}_4/\text{K}_2\text{HPO}_4$) recorded at $0.1 \text{ V} \cdot \text{s}^{-1}$ potential sweep rate on GC disk electrode at 298 K in the absence of DNA (a) and presence of 13 μM (b), 31 μM (c), 40 μM (d), 52 μM (e), and 56 μM DNA (f). Inset: plots of $1/1 - (j/j_0)$ vs. $1/[DNA]$ used to calculate the binding constant of ligand FMA with DNA

The decrease in anodic peak current density of the ligand FMA in the presence of DNA can be exploited for the calculation of the binding constant, while the shift in peak potential values can be used for the determination of the type of interaction [32, 33].

Binding constant of FMA with DNA was determined from the decline in the anodic peak current density of FMA-DNA adduct relative to free FMA using Eq. (1) [34]:

$$\frac{1}{[DNA]} = \frac{K(1-A)}{1 - (j/j_0)} - K \quad (1)$$

where $[DNA]$ is the DNA concentration, μM ; K represents the binding constant, M^{-1} ; j_0 and j denote the anodic peak current density of the free and DNA-bound ligand, respectively, $\mu\text{A}\cdot\text{cm}^{-2}$.

The binding energy ΔG was calculated using Eq. (2) [35]:

$$\Delta G = -RT \ln K \quad (2)$$

where ΔG is the binding free energy, $\text{kJ}\cdot\text{mol}^{-1}$, R is the gas constant, $8.32 \text{ J}\cdot\text{mol}^{-1}\text{K}^{-1}$; T is the absolute temperature equal to 298 K.

The equation obtained from the linear regression graph in the studied concentration range and DNA binding data of FMA are listed in Table 1.

Table 1

Binding constant and binding free energy values for FMA ligand with DNA from CV data at pH = 7.2 and $T = 298 \text{ K}$

Adduct	Equation	R^2	K, M^{-1}	$-\Delta G, \text{kJ}\cdot\text{mol}^{-1}$
FMA-DNA	$y = 1.3935x + 3.7157$	0.995	$5.2 \cdot 10^3$	21.21

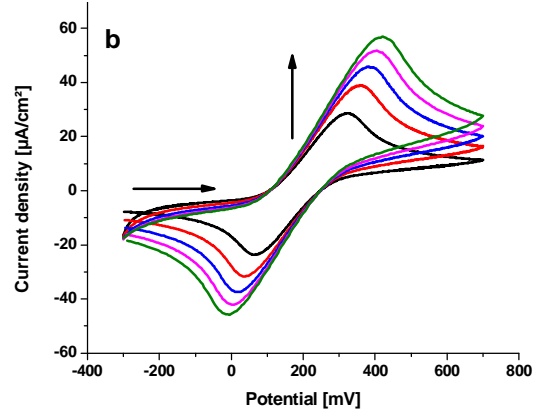
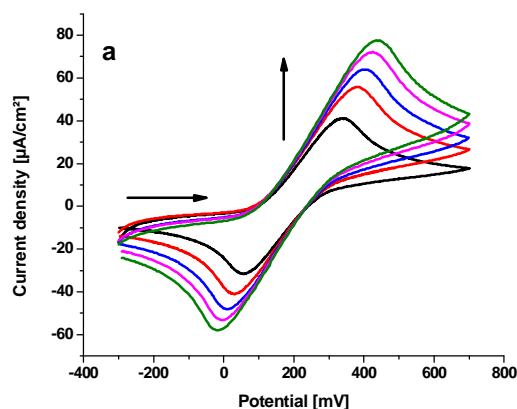
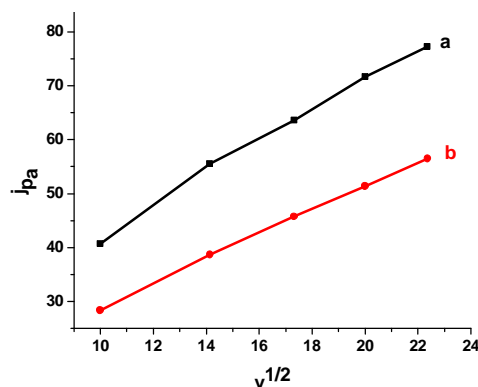


Fig. 3. Cyclic voltammetric behavior of 500 μM FMA on GC electrode in the absence (a) and presence of 63 μM (b) DNA in 0.1M aqueous buffer phosphate solution ($\text{KH}_2\text{PO}_4/\text{K}_2\text{HPO}_4$) at pH = 7.2 and scans rates 0.5, 0.4, 0.3, 0.2, and 0.1 $\text{V}\cdot\text{s}^{-1}$. The vertical arrowhead indicates increasing scan rate

Fig. 4. j vs. $v^{1/2}$ plots of FMA (500 μM) in the absence of DNA (a) and presence of 63 μM DNA (b) at scan rates ranging from 0.1 to 0.5 $\text{V}\cdot\text{s}^{-1}$ under the experimental conditions listed in Fig. 3



As can be seen from Table 1, the moderate ΔG value for the ligand FMA indicates their electrostatic mode of interaction with DNA; the sign of ΔG also points out to the spontaneity of ligand DNA interaction.

It has been reported that the electrostatic interaction of ligands with DNA might lead to conformational modifications in DNA, provoking perturbation in its normal functioning [36, 37]. This can presumably lead to the prevention of DNA duplication and functioning, and eventual cell death [38].

3.1.2. Diffusion coefficients

Fig. 3 shows the electrochemical behavior of the compound FMA at different scan rates. The voltammograms displayed clear stable anodic peaks. The diffusion coefficients of the free and DNA bound form of FMA were determined using the following Randles-Sevcik equation (3) [39].

$$j = 2.69 \cdot 10^5 n^{\frac{3}{2}} S C D^{\frac{1}{2}} v^{\frac{1}{2}} \quad (3)$$

where j is the peak current density, A; n is the number of electrons transferred during the oxidation; S is the surface area of the electrode, cm^2 ; C is the bulk concentration of the electro-active species, $\text{mol}\cdot\text{cm}^{-3}$; D is the diffusion coefficient, $\text{cm}^2\cdot\text{s}^{-1}$; v is the scan rate, $\text{V}\cdot\text{s}^{-1}$.

Table 2

Diffusion constants values of the free and DNA bound form of FMA

Compound	Equation	R^2	$D, \text{cm}^2 \cdot \text{s}^{-1}$
FMA	$y = 2.938x + 12.498$	0.992	$17.79 \cdot 10^{-5}$
FMA-DNA	$y = 2.269x + 6.155$	0.998	$10.56 \cdot 10^{-5}$

The plot of the square root of the scan rates versus the anodic peak current density (Fig. 4), suggests that the redox process is diffusion controlled. The values of the diffusion coefficients of the free and DNA-bound ligand were deduced from the slopes of the linear regression of Eq. (3). The lower diffusion coefficient of the bounded ligand as compared to the free ligand further suggests the adduct formation (Table 2).

The linearity of the relation $j_{pa} = f(v^{1/2})$ for both FMA and FMA-DNA suggests that the redox process is kinetically controlled by the diffusion step. The diffusion coefficients were determined from the slopes of Randles-Sevcik plots. Values are given in Table 2. It can be seen that the diffusion coefficient of DNA bound FMA is slightly lower than that of the free FMA. The lower diffusion coefficient of FMA-DNA can be attributed to the large molecular weight of the adduct FMA-DNA, which causes the decrease in the apparent diffusion coefficient of DNA in the occurrence of FMA.

3.2. UV-Visible Spectroscopic Studies

The interaction of FMA with DNA was also studied by electronic spectroscopy titration method, where 1 mM of FMA in buffer phosphate solution ($\text{KH}_2\text{PO}_4/\text{K}_2\text{HPO}_4$) at pH 7.2 was subjected to an increasing concentration of DNA. The UV-visible behavior of the ligand FMA on addition of gradually increasing concentration of DNA solution is presented in Fig. 5, which illustrates that the absorbance of FMA at 435 nm diminishes with the gradual increase of DNA concentration. At the same time, the maximum wavelength of ligand FMA increases initially and then becomes almost constant as shown by the loose curve in Fig. 5.

The change in absorbance values by increasing DNA concentration was used to evaluate the intrinsic binding constant employing Eq. (4) [39, 40].

$$\frac{A_0}{A - A_0} = \frac{e_G}{e_{H-G} - e_G} + \frac{e_G}{e_{H-G} - e_G} \frac{1}{K [DNA]} \quad (4)$$

Binding constant and binding free energy values for FMA compound with DNA from UV-visible spectrophotometric data at pH = 7.2 and 298 K

Adduct	Equation	R^2	K, M^{-1}	$-\Delta G, \text{kJ} \cdot \text{mol}^{-1}$
FMA-DNA	$y = -170.189x - 0.786$	0.904	$4.6 \cdot 10^3$	20.92

where $[DNA]$ is the DNA concentration, μM ; K is the binding constant, M^{-1} ; A_0 and A are the absorbance of ligand in the absence and presence of DNA, respectively, and e_G and e_{H-G} are their respective extinction coefficients, $\text{M}^{-1} \cdot \text{cm}^{-1}$.

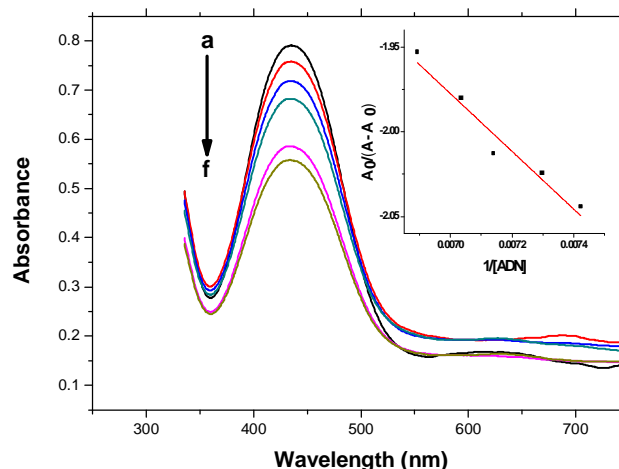


Fig. 5. UV-Vis absorption spectra of 1 mM of FMA in 0.1M buffer phosphate solution ($\text{KH}_2\text{PO}_4/\text{K}_2\text{HPO}_4$) at pH = 7.2 and 298 K in the absence of DNA (a) and presence of 26 μM (b), 41 μM (c), 55 μM (d), 83 μM (e), and 92 μM (f) of DNA. Inset: Plots of $A_0 / (A - A_0)$ vs. $1 / [DNA]$ used to calculate the binding constant of ligand-FMA with DNA

The constant K is obtained from the intercept to slope ratio of the plot of $A_0 / (A - A_0)$ versus $1 / [DNA]$. The plot of $A_0 / A - A_0$ versus $1 / [DNA]$ gave a slope and the y-intercept which are equal to $e_G / (e_{H-G} - e_G)K$ and $e_G / e_{H-G} - e_G$, respectively. The binding constant K was obtained from the ratio of the slope to the intercept and is reported in Table 3. The DNA binding constant obtained from UV-visible measurements are in good agreement with that obtained from CV studies.

Table 3

3.3. Molecular Docking Studies

In order to elucidate and validate the results obtained from voltammetric and spectroscopic measurements and to explore additional information of the ligand conformation and its orientation in the active site of the receptor, the interaction of ligand FMA with DNA were simulated by molecular docking; the docking also allows visualizing the intercalation pattern of the ligand with DNA.

3.3.1. Structural optimization

The chemical structure of FMA was optimized by Gaussian 09 program package [41], using the B3LYP level of theory [42, 43] with 6-311++G(d,p) basis set. Geometries of the complexes were fully optimized by employing the density functional theory, without imposing any symmetry constraints. Fig. 6 shows optimized structure of studied ligand.

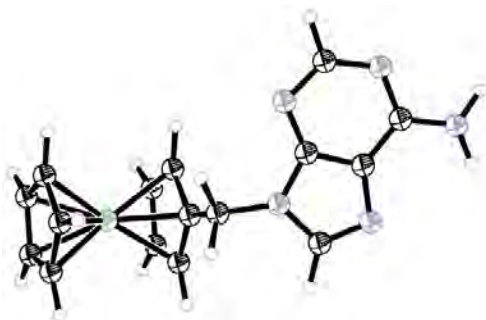


Fig. 6. 3D conformation of ligand FMA (ORTEP View 03, V1.08); thermal ellipsoids are plotted at the 50 % probability level

3.3.2. Docking simulations

The molecular docking studies of FMA ligand into DNA were carried out using AutoDock 4.2 docking software [44]. The optimized structures of FMA and DNA were imported to the AutoDock molecular docking

software. All docking studies were carried out on a Pentium 3.30 GHz and RAM 4.00 Go microcomputer MB memory with Windows 7 operating system.

The crystal structure of the synthetic DNA dodecamer (CpGpCpGpApApTpTpCpGpCpG) (PDB ID: 1BNA) selected from protein data bank (<http://www.rcsb.org/pdb>) [45] was chosen as the receptor to study binding of the ligand FMA. For the DNA structure, all hydrogen atoms and gasser charges were added to the DNA for docking simulation analysis and non-polar hydrogen atoms were merged. For docking calculations, Lamarckian genetic algorithms were used, and grid size was set at 50×50×50 with point separated by 1.000 Å. The grid centers were set at $X = 14.78$, $Y = 20.976$ and $Z = -8.807$. The docking experiment consisted of 25 docking runs with 150 individuals and 2500000 energy evaluations. Other parameters were left to their default values. The search was conducted in a grid of 50 points per dimension and the step size of 0.375 centered on the binding site of DNA. The best conformation was selected with the lower docking energy [46].

At the end of docking runs, diverse binding energies of the ligand were obtained with their respective conformations; the stable conformation, which corresponds to the lowest binding energy, was chosen as the best pose and was used in the docking analysis.

The binding energy of the docked structure of the FMA ligand with DNA was found to be $-22.28 \text{ kJ}\cdot\text{mol}^{-1}$ at the 3rd run. The magnitude of the calculated binding energy indicates a high binding affinity between DNA and the studied ligand (Table 4). The binding constant K was calculated using Eq. (2).

Table 4

Binding constant and binding free energy values obtained for FMA -DNA adduct by molecular docking approach

$-\Delta G, \text{kJ}\cdot\text{mol}^{-1}$	22.28
K, M^{-1}	$7.9\cdot 10^3$

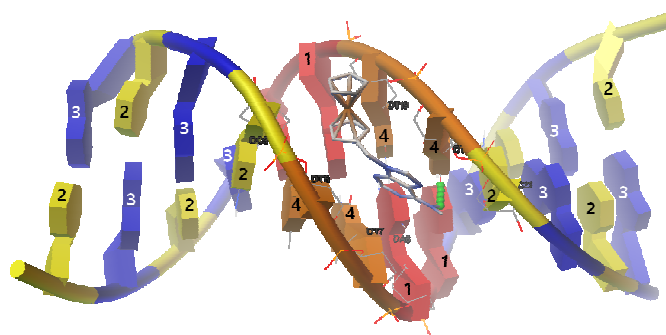


Fig. 7. Docking pose of FMA with DNA (PDB ID : 1BNA) illustrating the interactions between DNA and FMA: DA (1); DC (2); DG (3) and DT (4)

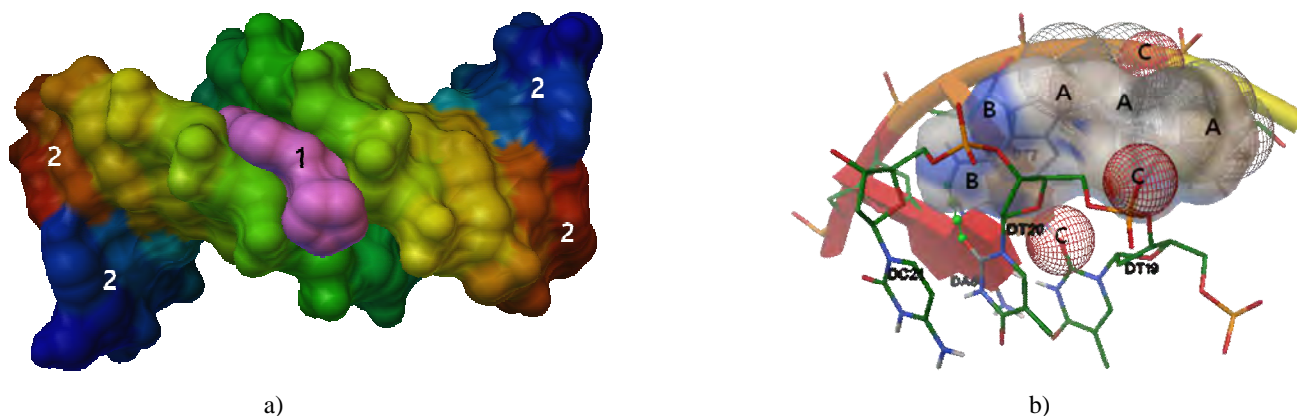


Fig. 8. Surface view (a) of docked FMA (1) with DNA (2) and three-dimensional model (b) of interactions of FMA with DNA, the DNA is presented by secondary structure and by CPK, and by lines denoted by atom type: carbon (A); polar hydrogen (B) and oxygen (C). FMA is depicted by sticks and balls

The results indicate that the ligand FMA interact with DNA by the hydrogen atom of the amine function *via* hydrogen bond to the oxygen atom number 2 of the nucleoside DT20 (Fig. 7).

The docking study on the FMA-DNA system showed that the FMA is placed in the minor groove of DNA. Fig. 8a shows the surface view of the docked conformation, indicating that ligand FMA fits well in the minor groove of DNA. Fig. 8b shows the close-up sight of the atoms of nucleotides of DNA interacting with the surface of FMA. It can be seen that the oxygen atom (O2) of the base pair deoxythymidine-20 (DT20) is interacting electrostatically with the hydrogen atom of FMA.

4. Conclusions

Voltammetric and spectroscopic assays accompanied by molecular docking calculations were used to study the interaction of 9*N*-(ferrocenylmethyl)adenine with DNA. The experimental results and molecular docking studies indicate that 9*N*-(ferrocenylmethyl)adenine possesses significant binding affinity with DNA via electrostatic interactions as the dominant mode. Furthermore, the order of magnitude of binding energy confirms the electrostatic interaction of 9*N*-(ferrocenylmethyl)adenine with DNA. These findings clearly indicate that the studied ligand can cause conformational changes in the structure of DNA, subsequently slowing down the cell replication process and eventually preventing the cell death.

Acknowledgements

The authors are grateful to the Algerian Ministry of Higher Education and Research for financial support

(project code: B00L01UN390120150001). We would also like to thank Mr Ali Tliba (VTRS staff) for his help.

References

- [1] Kealy T., Pauson P.: *Nature*, 1951, **168**, 1039. <https://doi.org/10.1038/1681039b0>
- [2] Miller S., Tebboth J., Tremaine J.: *J. Chem. Soc.*, 1952, **632**. <https://doi.org/10.1039/JR9520000632>
- [3] Wilkinson G., Rosenblum M., Whiting M. *et al.*: *J. Am. Chem. Soc.*, 1952, **74**, 2125. <https://doi.org/10.1021/ja01128a527>
- [4] Xian-Feng H., Ling-Zhu W., Long T. *et al.*: *J. Organomet. Chem.*, 2014, **749**, 157. <https://doi.org/10.1016/j.jorganchem.2013.08.043>
- [5] Lal B., Badshah A., Altaf A. *et al.*: *Dalton. Trans.*, 2012, **41**, 14643. <https://doi.org/10.1039/C2DT31570J>
- [6] Ornelas C.: *New J. Chem.*, 2011, **35**, 1973. <https://doi.org/10.1039/C1NJ20172G>
- [7] Kondapi A., Satyanarayana N., Saikrishna A.: *Arch. Biochem. Biophys.*, 2006, **450**, 123. <https://doi.org/10.1016/j.abb.2006.04.003>
- [8] Struga M., Kossakowski J., Kedzierska E. *et al.*: *Chem. Pharm. Bull.*, 2007, **55**, 796. <https://doi.org/10.1248/cpb.55.796>
- [9] Biot B., Francois N., Maciejewski L. *et al.*: *Bioorg. Med. Chem. Lett.*, 2000, **10**, 839. [https://doi.org/10.1016/S0960-894X\(00\)00120-7](https://doi.org/10.1016/S0960-894X(00)00120-7)
- [10] Itoh T., Shirakami S., Ishida N. *et al.*: *Bioorg. Med. Chem. Lett.*, 2000, **10**, 1657. [https://doi.org/10.1016/S0960-894X\(00\)00313-9](https://doi.org/10.1016/S0960-894X(00)00313-9)
- [11] Swarts J., Vosloo T., Cronge S. *et al.*: *Anticancer Res.*, 2008, **28**, 2781.
- [12] Acevedo-Morantes C., Meléndez E., Singh P. *et al.*: *J. Cancer. Sci. Ther.*, 2012, **4**, 271. <https://doi.org/10.4172/1948-5956.1000154>
- [13] Morad M., Sarhan A.: *Science*, 2008, **50**, 744. <https://doi.org/10.1016/j.corsci.2007.09.002>
- [14] Gupta S., Mourya P., Singh M. *et al.*: *J. Organomet. Chem.*, 2014, **767**, 136. <https://doi.org/10.1016/j.jorganchem.2014.05.038>
- [15] Van Staveren D., Metzler-Nolte N.: *Chem. Rev.*, 2004, **104**, 5931. <https://doi.org/10.1021/cr0101510>
- [16] Fouda M., Abd-Elzaher M., Abdelsamaia R. *et al.*: *Appl. Organomet. Chem.*, 2007, **21**, 613. <https://doi.org/10.1002/aoc.1202>

- [17] Lal B., Badshah A., Altaf A. *et al.*: Dalton. Trans., 2012, **41**, 14643. <https://doi.org/10.1039/C2DT31570J>
- [18] Scaria V., Furlani A., Longato B. *et al.*: Inorg. Chim. Acta, 1988, **153**, 67. [https://doi.org/10.1016/S0020-1693\(00\)83359-9](https://doi.org/10.1016/S0020-1693(00)83359-9)
- [19] Neuse E., Meirim M., Blom N.: Organometallics, 1988, **7**, 2562. <https://doi.org/10.1021/om00102a023>
- [20] Houlton A., Roberts R., Silver J.: J. Organomet. Chem., 1991, **418**, 107. [https://doi.org/10.1016/S1387-1609\(00\)00118-3](https://doi.org/10.1016/S1387-1609(00)00118-3)
- [21] Houlton A., Christian J., Ashleigh E. *et al.*: J. Chem. Soc., Dalton Trans., 1999, 3229. <https://doi.org/10.1039/A905168F>
- [22] Price C., Aslanoglu M., Christian J. *et al.*: J. Chem. Soc., Dalton Trans., 1996, 4115. <https://doi.org/10.1039/DT9960004115>
- [23] Ali S., Badshah A., Ataf A.: Med. Chem Res., 2013, **22**, 3154. <http://dx.doi.org/10.1007/s00044-012-0311-8>
- [24] Hussain R., Badshah A., Tahir M. *et al.*: Aust. J. Chem., 2013, **66**, 626. <https://doi.org/10.1071/CH12570>
- [25] Jalali F., Dorraji P.: J. Pharm. Biomed. Anal., 2012, **70**, 598. <https://doi.org/10.1016/j.jpba.2012.06.005>
- [26] Radi A., Eissa A., Nassef H.: J. Electroanal. Chem., 2014, **717**, 24. <https://doi.org/10.1016/j.jelechem.2014.01.007>
- [27] Osgerby J., Pauson P.: J. Chem. Soc., 1958, **642**, 656. <https://doi.org/10.1039/JR9580000656>
- [28] Snegur L., Yu S., Nekrasov N. *et al.*: Appl. Organomet. Chem., 2008, **22**, 139. <https://doi.org/10.1002/aoc.1362>
- [29] Sambrook J., Fritsch E., Maniatis T.: Molecular Cloning: A Laboratory Manual, 2nd edn., Cold Spring Harbour Laboratory Press, New York 1989, 1626-1644.
- [30] Glasel J.: Biotechniques, 1995, **8**, 62.
- [31] Vijayalakshmi R., Kanthimathi M., Subramanian V. *et al.*: Biochem. Biophys. Res. Commun., 2000, **271**, 731. <https://doi.org/10.1006/bbrc.2000.2707>
- [32] Lu X., Zhu K., Zhang M. *et al.*: J. Biochem. Biophys. Met., 2002, **52**, 189.
- [33] Aslanoglu M., Ayne G.: Anal. Bioanal. Chem., 2004, **380**, 658. <https://doi.org/10.1007/s00216-004-2797-5>
- [34] Zhao G., Zhu J., Zhang J. *et al.*: Anal. Chim. Acta., 1999, **394**, 337. [https://doi.org/10.1016/S0003-2670\(99\)00292-5](https://doi.org/10.1016/S0003-2670(99)00292-5)
- [35] Atkins P.: Physical Chemistry. Oxford University Press, Oxford 1986, 263-265.
- [36] Xu Z., Bai G., Dong C.: Bioorg. Med. Chem., 2005, **13**, 5694. <https://doi.org/10.1016/j.bmc.2005.06.023>
- [37] Ye H., Cande C., Stephanou N.: Nat. Struct. Mol. Biol., 2002, **9**, 680. <https://doi.org/10.1038/nsb836>
- [38] Li D., Huang F., Chen G. *et al.*: J. Inorg. Biochem., 2010, **104**, 431. <https://doi.org/10.1016/j.jinorgbio.2009.12.008>
- [39] Brett C., Brett A.: Electrochemistry: Principles, Methods and Applications, Oxford Science University Publications, Oxford 1993, 256-276.
- [40] Nie M., Wang Y., Li H.: Pol. J. Chem., 1997, **71**, 816.
- [41] Frisch M., Trucks G., Schlegel H. *et al.*: Gaussian 09. Gaussian Inc., Wallingford CT, 2009.
- [42] Becke A.: J. Chem. Phys., 1993, **98**, 5648. <https://doi.org/10.1063/1.464913>
- [43] Miehlisch B., Savin A., Stoll H. *et al.*: Chem. Phys. Lett., 1989, **157**, 200. [https://doi.org/10.1016/0009-2614\(89\)87234-3](https://doi.org/10.1016/0009-2614(89)87234-3)
- [44] Morris G., Ruth H., Lindstrom W. *et al.*: J. Comput. Chem., 2009, **30**, 2785. <https://doi.org/10.1002/jcc.21256>
- [45] Berman H., Westbrook J., Feng Z. *et al.*: Nucl. Acids Res., 2000, **28**, 235.
- [46] Lanez T., Benaicha H., Lanez E. *et al.*: J. Sulfur Chem., 2018, **39**, 76. <https://doi.org/10.1080/17415993.2017.1391811>

Received: November 02, 2017 / Revised: November 09, 2017 / Accepted: January 25, 2018

ОБЧИСЛОВАЛЬНИЙ МОЛЕКУЛЯРНИЙ ДОКІНГ, ВОЛТАМЕТРИЧНІ ТА СПЕКТРОСКОПІЧНІ ДОСЛІДЖЕННЯ ВЗАЄМОДІЇ ДНК З 9N-(ФЕРРОЦЕНІЛМЕТИЛ)АДЕНІНОМ

Анотація. З використанням методів циклічної вольтамперометрії та електронної спектроскопії за однакових умов проведені вимірювання вільної енергії 9N-(ферроценілметил)аденину (ФМА) з дволанцюговою ДНК. Отримані результати підтверджені обчислювальним молекулярним докінгом. Показано, що док-результати добре узгоджуються з експериментальними даними і що ліганд ФМА поміщений у невелику борозенку спіралі ДНК.

Ключові слова: ДНК, енергія вільного зв'язування, AutoDock, розмір ділянки зв'язування, коефіцієнт дифузії.